Polarimetric study of birefringent turbid media with three-dimensional optic axis orientation

Noé Ortega-Quijano,[*] **Félix Fanjul-Vélez, and José Luis Arce-Diego**

Applied Optical Techniques Group, Electronics Technology, Systems and Automation Engineering Department,
University of Cantabria, Avenida de los Castros S/N, 39005 Santander, Cantabria, Spain
[*]*ortegan@unican.es*

Abstract: Recent approaches to the analysis of biological samples with three-dimensional linear birefringence orientation require numerical methods to estimate the best fit parameters from experimental measures. We present a novel analytical method for characterizing the intrinsic retardance and the three-dimensional optic axis orientation of uniform and uniaxial turbid media. It is based on a model that exploits the recently proposed differential generalized Jones calculus, remarkably suppressing the need for numerical procedures. The method is applied to the analysis of samples modeled with polarized sensitive Monte Carlo. The results corroborate its capacity to successfully characterize 3D linear birefringence in a straightforward way.

References and links

1. N. Ghosh and I. A. Vitkin, "Tissue polarimetry: concepts, challenges, applications, and outlook," J. Biomed. Opt. **16**(11), 110801 (2011).
2. F. Fanjul-Vélez and J. L. Arce-Diego, "Polarimetry of birefringent biological tissues with arbitrary fibril orientation and variable incidence angle," Opt. Lett. **35**(8), 1163–1165 (2010).
3. N. Ugryumova, S. V. Gangnus, and S. J. Matcher, "Three-dimensional optic axis determination using variable-incidence-angle polarization-optical coherence tomography," Opt. Lett. **31**(15), 2305–2307 (2006).
4. M. A. Wallenburg, M. F. G. Wood, N. Ghosh, and I. A. Vitkin, "Polarimetry-based method to extract geometry-independent metrics of tissue anisotropy," Opt. Lett. **35**(15), 2570–2572 (2010).
5. N. Ortega-Quijano and J. L. Arce-Diego, "Generalized Jones matrices for anisotropic media," Opt. Express **21**(6), 6895–6900 (2013).
6. N. Ortega-Quijano and J. L. Arce-Diego, "Mueller matrix differential decomposition," Opt. Lett. **36**(10), 1942–1944 (2011).
7. R. M. A. Azzam, "Three-dimensional polarization states of monochromatic light fields," J. Opt. Soc. Am. A **28**(11), 2279–2283 (2011).
8. C. R. Jones, "A new calculus for the treatment of optical systems. VII. Properties of the N-matrices," J. Opt. Soc. Am. **38**(8), 671–685 (1948).
9. S. Jiao and L. V. Wang, "Jones-matrix imaging of biological tissues with quadruple-channel optical coherence tomography," J. Biomed. Opt. **7**(3), 350–358 (2002).
10. S. Jiao and L. V. Wang, "Two-dimensional depth-resolved Mueller matrix of biological tissue measured with double-beam polarization-sensitive optical coherence tomography," Opt. Lett. **27**(2), 101–103 (2002).
11. D. Lara and C. Dainty, "Axially resolved complete Mueller matrix confocal microscopy," Appl. Opt. **45**(9), 1917–1930 (2006).
12. G. Yao and L. V. Wang, "Two-dimensional depth-resolved Mueller matrix characterization of biological tissue by optical coherence tomography," Opt. Lett. **24**(8), 537–539 (1999).
13. R. Barakat, "Exponential versions of the Jones and Mueller-Jones polarization matrices," J. Opt. Soc. Am. A **13**(1), 158–163 (1996).
14. N. Ortega-Quijano, B. Haj-Ibrahim, E. García-Caurel, J. L. Arce-Diego, and R. Ossikovski, "Experimental validation of Mueller matrix differential decomposition," Opt. Express **20**(2), 1151–1163 (2012).
15. N. Ortega-Quijano and J. L. Arce-Diego, "Depolarizing differential Mueller matrices," Opt. Lett. **36**(13), 2429–2431 (2011).
16. R. Ossikovski, "Differential matrix formalism for depolarizing anisotropic media," Opt. Lett. **36**(12), 2330–2332 (2011).
17. J. C. Ramella-Roman, S. A. Prahl, and S. L. Jacques, "Three Monte Carlo programs of polarized light transport into scattering media: part I," Opt. Express **13**(12), 4420–4438 (2005).

18. X. Wang and L. V. Wang, "Propagation of polarized light in birefringent turbid media: A Monte Carlo study," J. Biomed. Opt. **7**(3), 279–290 (2002).

1. Introduction

Polarization-sensitive optical techniques are receiving a growing interest for biological tissues characterization, as they provide additional contrast mechanisms for medical imaging [1]. Many biological tissues are anisotropic, being linear birefringence the main type of anisotropy mainly due to the ubiquitous presence of collagen in a wide range of tissues and organs. Therefore, accurate polarimetric characterization methods can take advantage of birefringence information for characterization and diagnostic purposes [1].

Most of the methods used for the polarimetric analysis of biological tissues are only valid when birefringence orientation is arranged parallel to the detection plane. Otherwise, effective values are obtained instead of the intrinsic ones [2–4]. Regarding the terminology used throughout this paper, it is important to highlight that the term effective has the same physical meaning as the "apparent" parameter used in [3,4], and the term intrinsic is equivalent to the "true" magnitude in [3] and the "reconstructed" parameter in [4]. A polarimetric model of birefringent media with arbitrary optic axis orientation was presented in [2], which is useful for tissues with varying polar angles such as articular cartilage. Some methods have been proposed for analyzing samples with three-dimensional linear birefringence orientation, namely the variable-incidence-angle method [3] and the dual-projection method [4]. However, in both of them the quantitative characterization of linear birefringence is based on numerical methods that obtain the best fit to experimental measures.

We present a novel method for determining the intrinsic retardance and the 3D optic axis orientation of uniform turbid media with uniaxial birefringence. The main advantage of our method (which also requires to characterize the sample at two different angles) is that full birefringence characterization is performed using an analytical procedure, and therefore does not require any numerical approach to estimate the best fit parameters. The method is based on the differential generalized Jones calculus recently proposed [5], which enables to obtain the theoretical differential Jones and Mueller-Jones matrices of a uniaxial medium with arbitrarily-oriented linear birefringence. We show that the combination of such information with the analysis of Mueller matrices using the differential decomposition [6] enables to accurately obtain the 3D orientation and intrinsic retardance of the medium in a straightforward way.

2. Differential Jones matrix of birefringent media with arbitrary optic axis orientation

First, we consider a transverse totally polarized light beam propagating along an arbitrary propagation direction $\hat{\mathbf{n}}$ in a right-handed *xyz* Cartesian coordinate system. Such beam is completely characterized by the 3×1 Generalized Jones Vector (GJV) [7], whose elements are the time-independent terms of the *x*, *y* and *z* electric field components. According to the differential Generalized Jones calculus [5], the evolution of the GJV $\vec{\mathbf{E}}$ along the propagation direction in a uniform medium is:

$$d\vec{\mathbf{E}}/dl = \mathbf{g}\vec{\mathbf{E}},\tag{1}$$

where $\mathbf{g}$ is the 3×3 differential Generalized Jones Matrix (dGJM) of the sample and l is the traveled distance. We have recently presented a general method for obtaining the dGJM of non-depolarizing uniaxial linear samples with arbitrary anisotropic properties [5]. The most general expression of the dGJM involves 18 differential parameters directly related to the complex propagation constant of the medium. If we consider the particular case of a uniaxial medium exhibiting linear retardance (LR) with the optic axis parallel to the *z* axis, we have previously shown [5] that the dGJM is a diagonal matrix given by:

$$\mathbf{g}_{\mathbf{LR}}^{z} = \left(1/\sqrt{3}\right)\eta_q^z\mathbf{O_4} = \mathrm{diag}\left(i\eta_q^z/3, i\eta_q^z/3, -i2\eta_q^z/3\right),\tag{2}$$

$\mathbf{O}_4$ being the following Gell-Mann matrix:

$$\mathbf{O}_4 = \left(1/\sqrt{3}\right)\mathrm{diag}\left(1,1,-2\right). \tag{3}$$

Parameter η_q^z is the intrinsic birefringence of the medium, which quantifies the difference between the extraordinary and ordinary propagation constants ($\eta_q^z \equiv \Delta\eta = \eta_e - \eta_o$, using the same notation for the propagation constant as the one originally chosen by Jones [8]). The dGJM of such type of sample when the optic axis is arbitrarily oriented is given by the following expression:

$$\mathbf{g}_{\mathbf{LR}} = \mathbf{C}(\theta,\phi)\cdot\mathbf{g}^{\mathbf{z}}_{\mathbf{LR}}\cdot\mathbf{C}^{-1}(\theta,\phi), \tag{4}$$

where θ and ϕ are the polar and azimuthal angles of the optic axis, and matrix $\mathbf{C}(\theta,\phi)$ is:

$$\mathbf{C}(\theta,\phi) = \begin{bmatrix} \sin\phi & \cos\theta\cos\phi & \sin\theta\cos\phi \\ -\cos\phi & \cos\theta\sin\phi & \sin\theta\sin\phi \\ 0 & -\sin\theta & \cos\theta \end{bmatrix}, \tag{5}$$

which implements the coordinate transformation according to the convention established in [7]. It should be noted that Eq. (4) was first applied in [5] to the GJM, but remains obviously valid to the dGJM, exactly in the same way as two-dimensional rotations in the Jones calculus [8]. The dGJM constitutes an extension of the differential Jones matrix $\mathbf{j}$ to the three-dimensional framework [5], being $\mathbf{j}$ the upper-left 2×2 block of $\mathbf{g}$:

$$\mathbf{j} = \begin{bmatrix} \mathbf{g}(1,1) & \mathbf{g}(1,2) \\ \mathbf{g}(2,1) & \mathbf{g}(2,2) \end{bmatrix}. \tag{6}$$

Therefore, the differential Jones matrix of a uniaxial medium with arbitrarily oriented linear birefringence can be obtained by extracting the upper-left block of $\mathbf{g}_{\mathbf{LR}}$ (given by Eq. (4)), which results in the following matrix:

$$\mathbf{j}_{\mathbf{LR}} = i \begin{bmatrix} \dfrac{\Delta\eta}{2}\left(\cos^2\phi\cos2\theta - \dfrac{1}{2}\cos2\phi + \dfrac{1}{6}\right) & -\Delta\eta\cos\phi\sin\phi\sin^2\theta \\ -\Delta\eta\cos\phi\sin\phi\sin^2\theta & \dfrac{\Delta\eta}{2}\left(\sin^2\phi\cos2\theta + \dfrac{1}{2}\cos2\phi + \dfrac{1}{6}\right) \end{bmatrix}. \tag{7}$$

3. Three-dimensional birefringence characterization from polarimetric measurements

The differential Jones matrix obtained in the previous Section enables to develop an analytical method to determine linear birefringence in a biological sample with arbitrarily oriented optic axis. Polarization-sensitive optical imaging techniques for the polarimetric characterization of biological tissues can provide the Jones matrix (e.g. Jones and Mueller-Jones PS-OCT [9,10]) or the Mueller matrix (e.g. Mueller confocal microscopy [11], Mueller PS-OCT [12]) of the sample. Regarding the former group, it is well-known that Jones matrices and non-depolarizing Mueller matrices constitute a unique equivalent representation of the sample, so the non-depolarizing Mueller matrix can be readily obtained from any measured Jones matrix [13]. Therefore, our method is based on Mueller matrix analysis, providing a unified approach to the problem.

According to the differential Mueller decomposition [6,14], the accumulated differential Mueller matrix $\mathbf{\bar{m}} = \mathbf{m}l$ of the sample is the matrix logarithm of its Mueller matrix:

$$\bar{\mathbf{m}} = \operatorname{logm}(\mathbf{M}), \tag{8}$$

which is valid for diagonalizable Mueller matrices. In general, the differential Mueller matrix of a depolarizing anisotropic sample involves a total of 16 differential parameters [15]. The non-depolarizing part of $\bar{\mathbf{m}}$ is its Minkowski antisymmetric component [16]:

$$\bar{\mathbf{m}}_{\mathbf{nd}} = \frac{1}{2}(\bar{\mathbf{m}} - \mathbf{G}\bar{\mathbf{m}}^{\mathrm{T}}\mathbf{G}), \tag{9}$$

where $\mathbf{G}$ is the Minkowski metric $\mathbf{G} = \operatorname{diag}(1, -1, -1, -1)$. The azimuthal orientation angle of linear birefringence is obtained as:

$$\varphi = \frac{1}{2}\operatorname{a\,tan}\left(\frac{\delta_u}{\delta_q}\right), \tag{10}$$

in which $\delta_q = \bar{\mathbf{m}}_{\mathbf{nd}}(3,4)$ and $\delta_u = -\bar{\mathbf{m}}_{\mathbf{nd}}(2,4)$. Effective linear retardance is given by:

$$\delta^{ef} = \left(\delta_q^2 + \delta_u^2\right)^{1/2}. \tag{11}$$

The correspondence between a differential Jones matrix and its equivalent non-depolarizing Mueller matrix is given by the following well-known relationship [13]:

$$\mathbf{m}_{\mathbf{nd}} = \mathbf{A}(\mathbf{j} \oplus \mathbf{j}^*)\mathbf{A}^{-1}, \tag{12}$$

where $\mathbf{A}$ is the conversion matrix [13]. Substituting Eq. (7) into (12), the accumulated differential Mueller matrix of the linear birefringent medium considered in this work is:

$$\bar{\mathbf{m}}_{\mathbf{LR}} = \begin{bmatrix} 0 & 0 & 0 & 0 \\ 0 & 0 & 0 & \delta\sin 2\phi \sin^2\theta \\ 0 & 0 & 0 & -\delta\cos 2\phi \sin^2\theta \\ 0 & -\delta\sin 2\phi \sin^2\theta & \delta\cos 2\phi \sin^2\theta & 0 \end{bmatrix}, \tag{13}$$

where $\delta = \Delta\eta l$ denotes the intrinsic retardance of the sample. We recall that matrix $\bar{\mathbf{m}}_{\mathbf{LR}}$ is defined in the xy plane of the laboratory reference system. Following Eq. (11), the effective linear retardance is given by:

$$\delta^{ef} = \delta\sin^2\theta. \tag{14}$$

It can be observed that the effective linear retardance is not equal to the intrinsic linear retardance of the sample unless the optic axis is parallel to the detector xy plane (i.e. $\theta = 90º$). Although this critical issue is well-known, to the best of the Authors' knowledge the correspondence between the effective and intrinsic linear retardances has not been analytically stated before in the clear and precise terms of Eq. (14). From this expression, an analytical method for determining the magnitude and orientation of linear birefringence can be proposed. The first step of the method is to measure the Mueller matrix of the sample at two different incidence angles of the probing beam, denoted χ_1 and χ_2. In this sense, the proposed method requires the same experimental geometry as the variable-incidence-angle method [3] and the dual-projection method [4]. In this work we use the same notation for the incidence angle as the latter. The analysis of both experimental Mueller matrices following the procedure described above gives two effective linear retardances:

$$\begin{aligned} \delta_1^{ef} &= \delta \sin^2(\theta - \chi_1) \\ \delta_2^{ef} &= \delta \sin^2(\theta - \chi_2) \end{aligned} \tag{15}$$

From these magnitudes, the polar angle can be obtained by:

$$\theta = a \tan \left[\frac{D \sin \chi_2 - \sin \chi_1}{D \cos \chi_2 - \cos \chi_1} \right], \tag{16}$$

where $D = \left(\delta_1^{ef} / \delta_2^{ef} \right)^{1/2}$. Regarding the azimuthal angle, it is readily determined from a single Mueller matrix by Eq. (10). Finally, once the linear birefringence polar angle is known, the intrinsic retardance can be calculated as:

$$\delta = \frac{\left(\delta_1^{ef} \delta_2^{ef} \right)^{1/2}}{\sin(\theta - \chi_1) \sin(\theta - \chi_2)}. \tag{17}$$

For those techniques in which the optical path undergone by the measured photons could be precisely determined, the intrinsic birefringence would be obtained as $\Delta \eta = \delta / l$.

4. Application to tissue-like samples modeled by polarization sensitive Monte Carlo

The method proposed above is now applied to the analysis of uniaxial linear birefringent turbid samples modeled by the polarized light Monte Carlo method [17] including anisotropy [18] in transmission configuration. The procedure requires to first calculate the accumulated differential Mueller matrix from the original Mueller matrix provided by the Monte Carlo method, and subsequently follow the proposed method to obtain the azimuthal and polar angles and the intrinsic retardance that completely characterize the sample birefringence.

We have considered a wavelength of 632.8 nm. The medium refractive index is 1.341, and the sample length is 1 mm. Spherical scattering particles with a diameter of 1 μm and refractive index 1.59 have been modeled using Mie theory. The calculated scattering coefficient is 64.59 cm^{-1}, with a scattering anisotropy of 0.92. The refractive index difference along the extraordinary and the ordinary axes is $1.5 \cdot 10^{-4}$. We have considered four azimuthal angles of the optic axis (0°, 30°, 60° and 90°), and the polar angle was varied between 0° and 90° in steps of 10° for each of them. Regarding the measurement geometry, Mueller matrices are obtained for normal incidence ($\chi_1 = 0°$) and oblique incidence ($\chi_2 = 5°$) of the incoming beam. A minimum of 10^5 photons were detected in transmission for each simulation.
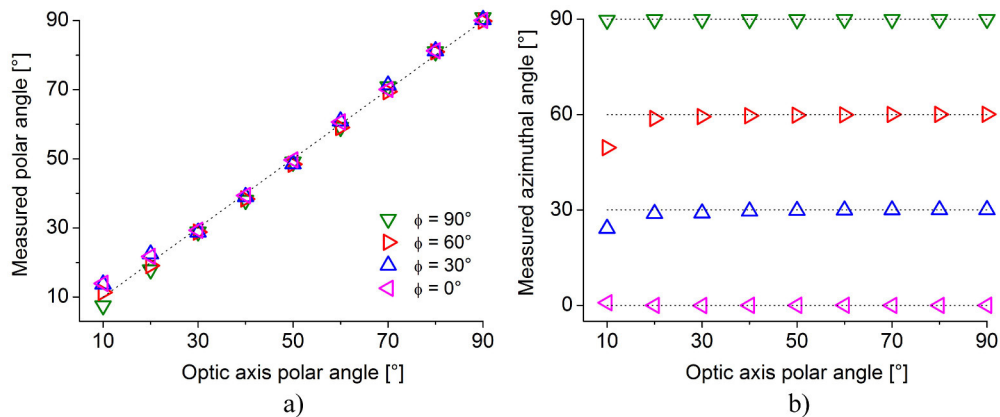

Fig. 1. a) Measured polar angles of the optic axis for all the samples. b) Measured optic axis azimuthal angles. In both cases, the dotted lines are where the calculated values should fall on.

The optic axis polar angle is first calculated following the procedure described in the previous Section. The results are presented in Fig. 1(a). The dotted line has been included to better compare the results with the input control values. The measured polar angles determined by our method follow the expected values, and the small deviations in the polar angles for the different azimuths corroborate the consistency of the results. Next, Fig. 1(b) shows the azimuthal angle determined for each sample. The agreement of the results with the theoretical control values is excellent in practically all the simulated samples. It can be observed that in both the polar and azimuthal angles the deviation from the nominal values increase for the smallest polar angles ($\theta = 10°$ and $20°$), which is due to the reduced accuracy when the optic axis is nearly orthogonal to the detection plane (i.e. nearly-isotropic situation).

Finally, once the optic axis orientation is known, we obtain the intrinsic retardance of the sample using Eq. (17). The results are depicted in Fig. 2 (diamonds), which represents the mean and standard deviation calculated for the four azimuthal angles considered. The retardance obtained when the optic axis is parallel to the detector xy plane has been taken as the intrinsic retardance control value (upper dotted line). Additionally, the effective retardance is included (squares), which perfectly corresponds to the expected behavior determined by Eq. (14) (lower dotted curve). Moreover, we note that these results are in agreement with those presented in [4], which reinforces the validity of our analytical method. It can be appreciated that the method successfully determines the intrinsic retardance of the samples, with a maximum calculated relative error of 5.30% for polar angles greater than 30°. Regarding $\theta = 10°$ and $20°$, the relative errors are 31.22% and 12.05% respectively due to the experimental errors produced for the near-isotropic situation as pointed out above. As a comparison, the relative errors entailed by the corresponding effective retardance are 96.98% and 88.30%. These results corroborate the potential of the method proposed in this work.
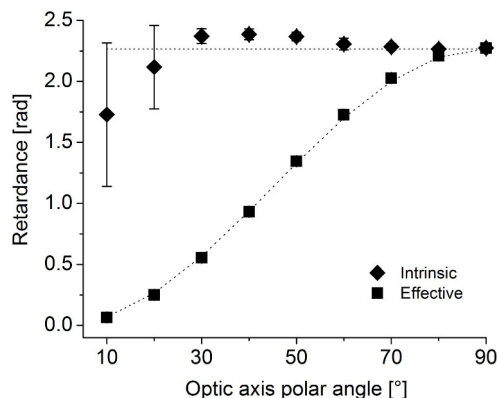

Fig. 2. Measured intrinsic (diamonds) and effective (squares) retardance. The dotted lines are where the calculated values should fall on. Results are averaged for the four azimuthal angles.

5. Conclusion

We have presented a novel method for the analysis of uniform turbid samples with arbitrarily-oriented uniaxial linear birefringence. The method takes advantage of the differential generalized Jones calculus, which enables to model the sample and interpret experimental results in a rigorous way. We have shown that the differential analysis of Mueller matrices measured at two different incidence angles enable to determine the intrinsic retardance and 3D orientation of the optic axis using analytical expressions. The procedure has been verified for birefringent turbid samples simulated with polarization sensitive Monte Carlo. Our method can be applied to a wide range of polarization-sensitive optical imaging techniques, and holds potential for further analyzing anisotropic tissue samples with simultaneous three-dimensional optical effects. Likewise, the method could be applied to the polarimetric analysis of a wide range of anisotropic media in other experimental fields.